Macromolecules

ARTICLE

pubs.acs.org/Macromolecules

Stimuli-Responsive Helical Poly(phenylacetylene)s Bearing Cyclodextrin Pendants that Exhibit Enantioselective Gelation in Response to Chirality of a Chiral Amine and Hierarchical Super-Structured Helix Formation

Katsuhiro Maeda,[†] Hiroaki Mochizuki, Keiko Osato, and Eiji Yashima*

Department of Molecular Design and Engineering, Graduate School of Engineering, Nagoya University, Chikusa-ku, Nagoya 464-8603, Japan

Supporting Information

ABSTRACT: Novel poly(phenylacetylene)s bearing a β-cyclodextrin (CyD) residue connected to the phenyl ring through an ester (poly-**2β**) and an ether linkage (poly-**3β**) as well as an amide linkage (poly-**1β**) were synthesized and their chiroptical properties were investigated with circular dichroism (CD) and absorption spectroscopies. The chiroptical studies demonstrated that the linkage groups play an important role in the conformational change induced by external chiral and achiral stimuli, such as temperature, solvent, and interactions with a chiral amine. Poly-**1β** and poly-**2β** showed a unique enantioselective gelation in response to the chirality of a chiral amine, and the polymers further formed hierarchical superstructured helical assemblies on a micrometer scale with a controlled helix sense, as evidenced by the scanning electron microscopy observations.

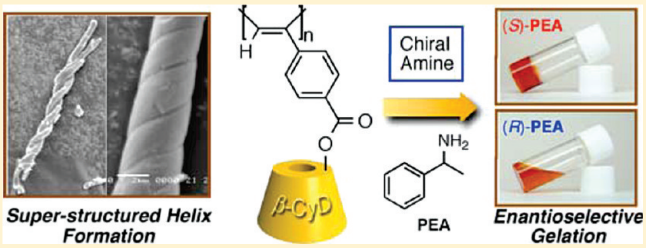

INTRODUCTION

Supramolecular self-assembly that results in the formation of helical aggregates, such as twisted ribbons, wires, fibers, and tubes, has been one of the emerging research topics that not only provides imagination to understanding and mimicking biological helices and superstructures but also creates functional nanomaterials for optoelectronic devices and biomaterials.[1] Although a huge number of helical assemblies have been constructed from small molecules through noncovalent bonding interactions,[2] only a few studies have reported supramolecular helical assemblies based on synthetic polymers, in particular, helical polymers except for biological polypeptides.[3,4]

We recently reported a unique helical polymer consisting of a chromophoric stereoregular (cis−transoidal) polyacetylene backbone and an optically active β-cyclodextrin (CyD) as the pendant groups linked through an amide bond (poly-**1β** in Chart 1), which showed a characteristic induced circular dichroism (ICD) in the π-conjugated polymer backbone regions.[5] The polymer also exhibited a visible color change due to a change in the twist angle of the conjugated polymer backbone induced by various external stimuli, such as the temperature, solvent, shape of the molecules, and chirality.[5,6] This visible color change was accompanied by inversion of the macromolecular helicity of the polymer backbone. We also synthesized a series of cis−transoidal poly(phenylacetylene)s bearing α- and γ-CyD (poly-**1α** and poly-**1γ**, respectively; Chart 1) and permethylated β-CyD residues and investigated the effect of the ring size of the CyD residues and the hydroxy groups in the CyD unit on their chiroptical properties including the macromolecular helicity inversion accompanied by a color change.[5,7]

Here we designed and synthesized novel CyD-bound poly(phenylacetylene)s bearing a β-CyD residue connected to the phenyl group through an ester (poly-**2β**) and an ether (poly-**3β**) linkage (Chart 1) instead of an amide linkage in poly-**1β** and investigated their chiroptical properties in solution by circular dichroism (CD) and absorption spectroscopies to evaluate the effects of the hydrogen-bonding ability and polarity of the linkages on their helical conformational changes responding to the external stimuli. During the course of our study, we unexpectedly discovered that poly-**1β** and poly-**2β** exhibited a unique enantioselective gelation in response to the chirality of a chiral amine, 1-phenylethylamine (**4**), and further hierarchically self-assembled to form a micrometer-scale, right-handed superstructured helix, as visualized by scanning electron microscopy (SEM). The effects of the ring size of the CyD residues and the linkage on the enantioselective gelation and supramolecular self-assembly of other CyD-bound poly(phenylacetylene)s were also investigated.

Received: March 9, 2011
Revised: April 3, 2011
Published: April 11, 2011

■ RESULTS AND DISCUSSION

Synthesis and Conformational Changes of Helical Poly-2β and Poly-3β in Response to Various Chiral and Achiral Stimuli. Stereoregular (cis−transoidal) poly-**2β** and poly-**3β** were prepared by the polymerization of the corresponding monomers with a rhodium catalyst using a method similar to that previously reported for poly-**1α**−poly-**1γ**,[7] as outlined in Scheme 1 in the Experimental Section, and their characteristics including poly-**1α**−poly-**1γ** are summarized in Table 1.[7] The cis−transoidal structures of poly-**2β** and poly-**3β** were confirmed by laser Raman spectroscopy (Figure S1 in the Supporting Information).

Poly-**2β** and poly-**3β** showed an intense CD in the long absorption regions of the polymer backbones at 25 °C in DMSO (Figures 1A and 2A, respectively), indicating a preferred-handed helix formation induced by the covalent-bonded chiral β-CyD units. Interestingly, the first Cotton effect sign of poly-**2β** that reflects the helix-sense of the polymer was opposite to those in poly-**1β** (Figure S2A in the Supporting Information) and poly-**3β** in DMSO.[7] This suggests that the helix-sense of poly-**2β** is opposite to that of poly-**1β** and poly-**3β**, regardless of the fact that the polymers have the same β-CyD pendant groups. As previously reported, poly-**1β** exhibited a color change from red to yellow in the presence of an increasing amount of water accompanied by inversion of the first Cotton effect from the negative to positive direction (Figure S2A,D in the Supporting Information).[7] Such a visible color change and the Cotton effect inversion in poly-**1β** can be ascribed to a change in the twist angle of the conjugated double bonds and an inversion of the helicity of the polymer backbone, respectively.[7,8]

Poly-**2β** and poly-**3β** showed a similar solvatochromism in DMSO in the presence of an increasing amount of water. The absorbance maximum (λ_{max}) at 510 nm of poly-**2β** blue-shifted

Chart 1. Structures of CyD-Bound Poly(phenylacetylene)s

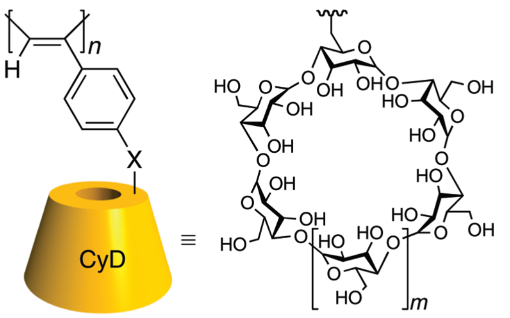

poly-**1β** (X = CONH, *m* = 2)
poly-**2β** (X = COO, *m* = 2)
poly-**3β** (X = O, *m* = 2)
poly-**1α** (X = CONH, *m* = 1)
poly-**1γ** (X = CONH, *m* = 3)

Table 1. CyD-Bound Poly(phenylacetylene)s Used in This Study

sample code	$M_n \times 10^{-4}$[a]	M_w/M_n[a]
poly-**1β**[b]	16.3	1.5
poly-**2β**	8.1	1.2
poly-**3β**	9.6	1.2
poly-**1α**[b]	16.0	1.2
poly-**1γ**[b]	11.1	1.2

[a] Number-average molecular weight (M_n) and its molecular weight distribution (M_w/M_n) were determined by size exclusion chromatography (SEC) using DMF containing 10 mM LiCl as the eluent with poly(ethylene oxide) (PEO) and poly(ethylene glycol) (PEG) standards. [b] Data are cited from ref 7.

Scheme 1. Synthesis of Poly-2β and Poly-3β

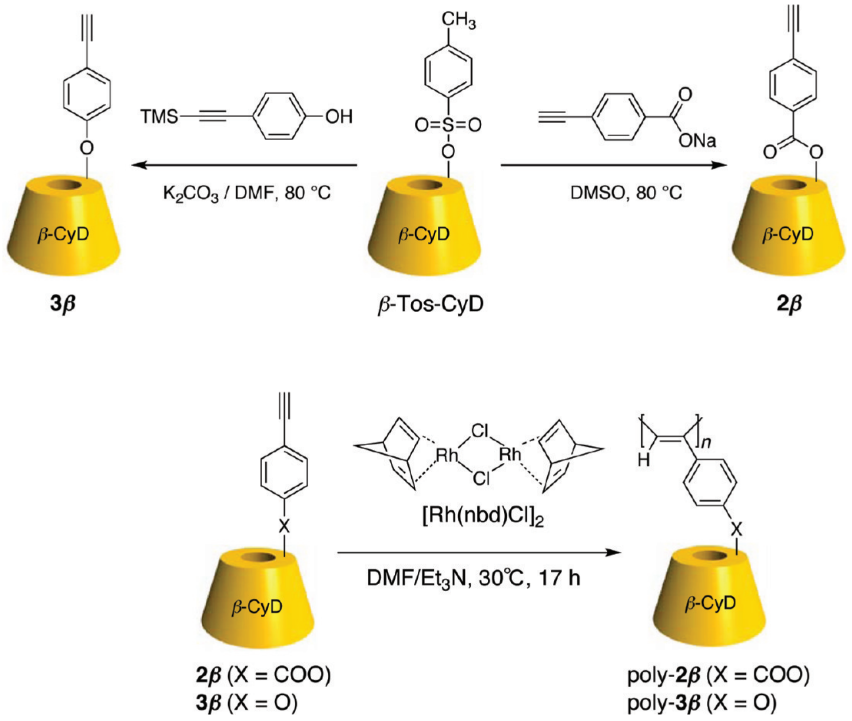

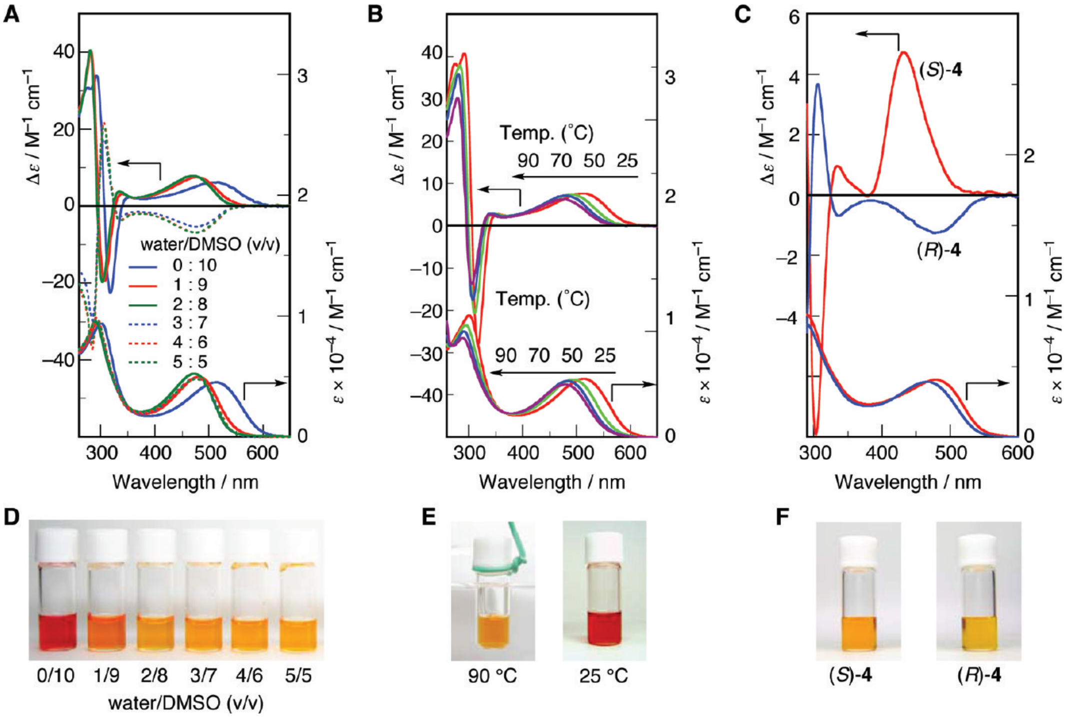

Figure 1. (A–C) CD and UV/vis spectra of poly-**2*β*** ([poly-**2*β***] = 1.0 mg/mL, 0.79 mM) in water/DMSO (5:5–0:10, v/v) at 25 °C (A), in DMSO at various temperatures (B), and in water/DMSO (6:4, v/v) in the presence of (*S*)-**4** (red lines) and (*R*)-**4** (blue lines) ([**4**] = 0.23 M) at 25 °C (C). The lines for water/DMSO (4:6 and 5:5, v/v) in (A) and those for water/DMSO (6:4, v/v) (data not shown) are almost overlapped. (D–F) Visible color changes of poly-**2*β*** in water/DMSO mixtures at ambient temperature (ca. 25 °C) (D) in DMSO at 90 (left) and 25 °C (right) (E) and in water/DMSO (6:4, v/v) with (*S*)- (left) and (*R*)-**4** (right) at ambient temperature (ca. 25 °C) (F).

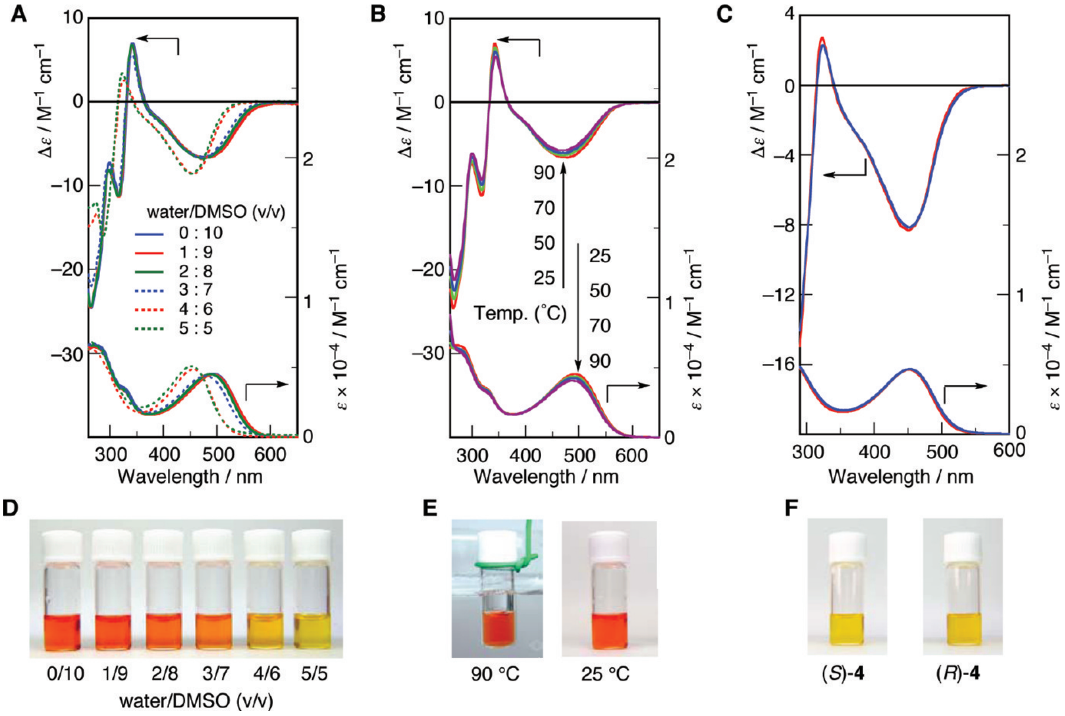

Figure 2. (A–C) CD and UV/vis spectra of poly-**3*β*** ([poly-**3*β***] = 1.0 mg/mL, 0.76 mM) in water/DMSO (5:5–0:10, v/v) at 25 °C (A), in DMSO at various temperatures (B), and in water/DMSO (5:5, v/v) in the presence of (*S*)-**4** (red lines) and (*R*)-**4** (blue lines) ([**4**] = 0.76 M) at 25 °C (C). (D–F) Visible color changes of poly-**3*β*** in water/DMSO mixtures at ambient temperature (ca. 25 °C) (D), in DMSO at 90 (left) and 25 °C (right) (E), and in water/DMSO (5:5, v/v) with (*S*)- (left) and (*R*)-**4** (right) at ambient temperature (ca. 25 °C) (F).

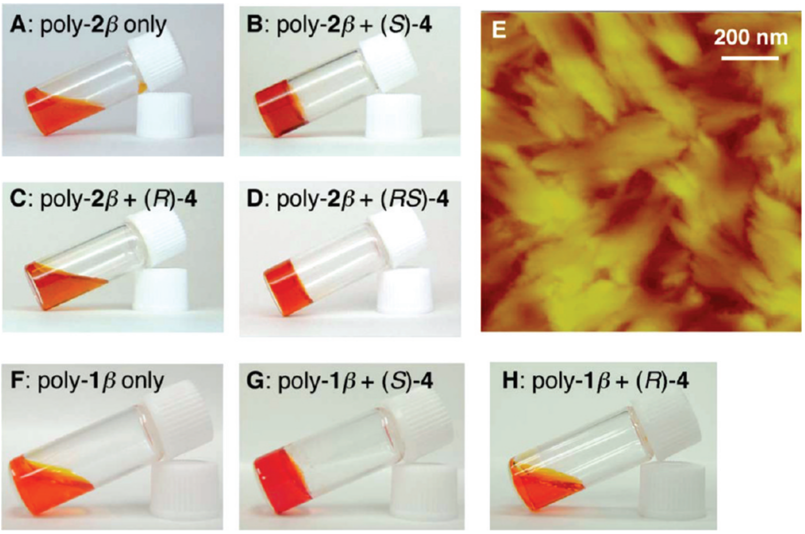

Figure 3. Enantioselective gelation of poly-**2*β*** and poly-**1*β*** upon the addition of chiral amine **4**. (A–D) Photographs of poly-**2*β*** (20 mg/mL) in the absence (A) and presence of (*S*)-**4** (B), (*R*)-**4** (C), and racemic (*RS*)-**4** (D) ([**4**]:[poly-**2*β***] 40:1, mol/mol) in water/DMSO (6:4, v/v) at room temperature. (E) AFM height image ($1.1 \times 1.1\ \mu m^2$) of the organogel composed of poly-**2*β*** and (*S*)-**4** (B) transferred on mica. (F–H) Photographs of poly-**1*β*** (20 mg/mL) in the absence (F) and presence of (*S*)-**4** (G) and (*R*)-**4** (H) ([**4**]:[poly-**1*β***] 40:1, mol/mol) in water/DMSO (6:4, v/v) at room temperature.

by 32 nm, and the solution color changed from red to yellow-orange accompanied by the inversion of the first Cotton effect sign from the positive to negative direction at around water/DMSO 3:7 (v/v) (Figure 1A,D). Poly-**3*β*** bearing an ether linker maintained its Cotton effect signs in the mixed solvents despite a similar blue shift in its absorption spectra, resulting in a visible color change (red to yellow) (Figure 2A,D). The blue shifts in the absorption spectra suggest that the polymers may have a more tightly twisted helical conformation in solution, whereas the red polymers may have an extended π-conjugation. Moreover, poly-**2*β*** also exhibited a clear thermochromism, as observed for poly-**1*β*** (Figure S2B,E in the Supporting Information); the λ_{max} significantly blue-shifted, and the solution color changed from red at 25 °C to yellow-orange at 90 °C (Figure 1B,E). However, the first Cotton effect sign of poly-**2*β*** remained positive even at high temperatures, although inversion of the Cotton effect took place for poly-**1*β*** accompanied by a change in the solution color (Figure S2B,E in the Supporting Information). In sharp contrast, the CD and absorption spectra of poly-**3*β***, in which the amide or ester linkage of poly-**1*β*** and poly-**2*β*** was replaced by an ether, in DMSO hardly changed upon heating; the solution remains red with a negative Cotton effect at 460 nm (Figure 2B,E). These results demonstrated that the linkage groups of the CyD-bound helical poly(phenylacetylene)s play an important role in the conformational change induced by external stimuli, which may be dictated by intramolecular hydrogen-bonding networks and dipole–dipole interactions of the pendant amide and ester groups of poly-**1*β*** and poly-**2*β***, respectively.

As previously reported, poly-**1*β*** discriminated the chirality of 1-phenylethylamine (**4**) and exhibited a CD inversion in the presence of (*S*)-**4** accompanied by a visible color change, whereas the poly-**1*β*** solution remained unchanged with a positive first Cotton effect (Figure S2C,F in the Supporting Information).[5,7,9] Poly-**2*β*** was also sensitive to the chirality of **4**, and (*S*)-**4** ([(*S*)-**4**]/[poly-**2*β***] = 300) induced an inversion in the Cotton effect signs in a mixture of water and DMSO (6/4, v/v). In the presence of (*R*)-**4** ([(*R*)-**4**]/[poly-**2*β***] = 300), however, the Cotton effect signs and absorption spectra did not change (Figure 1C). We note that the Cotton effect inversion of poly-**2*β*** with (*S*)-**4** was observed only in water/DMSO 6:4 (v/v) but did not take place in water/DMSO mixtures (5:5–0:10, v/v), indicating that the helical sense inversion appears to be governed by a delicate balance of specific interactions between poly-**2*β*** and **4** and also solvation with water. In contrast with poly-**1*β*** (Figure S2F in the Supporting Information), no apparent difference in the solution color was observed for poly-**2*β*** in the presence of either (*S*)-**4** or (*R*)-**4** (Figure 1F). Poly-**3*β*** bearing the same β-CyD units through an ether linkage showed negligible changes in the CD and absorption spectra independent of the configuration of **4** in water/DMSO mixtures (5:5–0:10) (for water/DMSO 5:5, see Figure 2C,F). These results suggest that a preferential chiral solvation with **4** on the polar amide and ester linkers rather than an enantioselective inclusion complexation of **4** in the β-CyD residues may be the driving force for the observed changes in the absorption and CD spectra and the solution color.

Enantioselective Gelation and Hierarchical Super-Structured Helix Formation. During the course of our study on chirality sensing, we unexpectedly discovered that poly-**2*β*** enantioselectively gelled only in the presence of (*S*)-**4** when the concentration was higher than 20 mg/mL (Figure 3).[10] Upon the addition of (*S*)-**4** ([(*S*)-**4**]/[poly-**2*β***] = 40), a solution of poly-**2*β*** (20 mg/mL) in a water/DMSO mixture (6:4, v/v) gradually gelled in a few minutes (Figure 3B), whereas the solution never gelled even in the presence of an excess amount of (*R*)-**4** (80 equiv) (Figure 3C). An atomic force microscopy (AFM) image of the ultrathin layer of the poly-**2*β*** gel with (*S*)-**4** obtained by transfer from the bulk gel surface onto highly oriented pyrolytic graphite (HOPG)[11] showed well-developed fibrous nanonetwork structures (Figure 3E), although the helically twisted structures could not be observed. Quite interestingly, the same solution also became a gel when the racemic **4** and nonracemic **4** rich in the (*S*)-enantiomer of 50% ee ([**4**]/[poly-**2*β***] = 40) were added (Figure 3D). These results suggest that (*R*)-**4** hardly

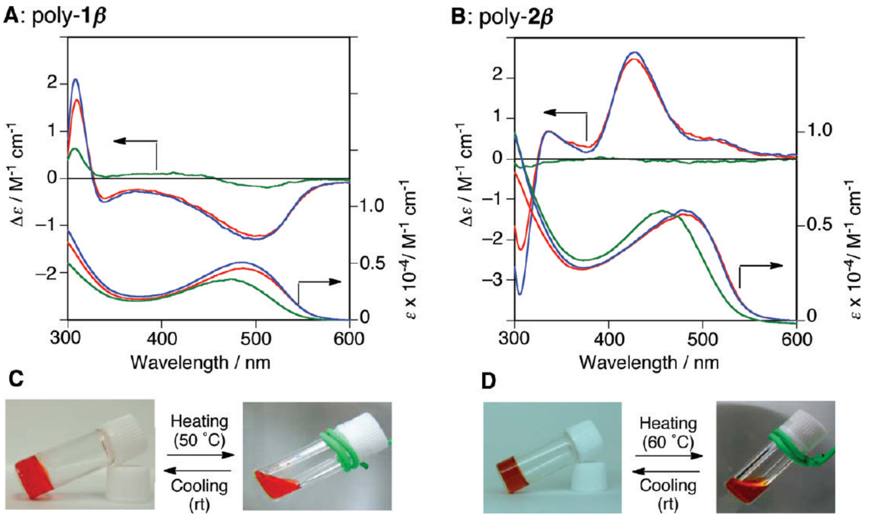

Figure 4. CD and absorption spectral changes of poly-**1*β*** (A) and poly-**2*β*** (B) with (*S*)-**4** ([(*S*)-**4**]/[poly-**2*β***] 40:1, mol/mol, [polymer] = 20 mg/mL) in water/DMSO (6:4, v/v). Photographs of poly-**1*β*** (C) and poly-**2*β*** (D) with (*S*)-**4** at room temperature before (red lines) and after (blue lines) heating at 50 (poly-**1*β***) and 60 °C (poly-**2*β***) (green lines).

contributes to the gelation, but poly-**2*β*** exclusively interacts with (*S*)-**4**, resulting in the gel. We also noted that (*S*)-**4** at >10 equiv is required for the gelation.

To gain insight into the mechanism of this unique enantioselective gelation of poly-**2*β***, we examined the effects of the water content in DMSO (water/DMSO = 0−100%, v/v) on the gelation in the presence of a constant concentration of (*S*)-**4** (40 equiv). Poly-**2*β*** solutions with (*S*)-**4** gelled within 0.5 h in the mixed solvents with water contents of >60 vol %, although a further increase in the water content (>90 vol %) caused a precipitation of the polymer (Table S1 in the Supporting Information).

We then investigated the gelation ability of a series of CyD-bound poly(phenylacetylene)s (poly-**1*β***, poly-**3*β***, poly-**1α**, and poly-**1*γ***) in water/DMSO mixed solvents under the same experimental conditions. A similar enantioselective gelation took place for poly-**1*β*** in response to the chirality of **4**, although a rather longer time (∼2 days) was required for the gelation (Table S1 in the Supporting Information and Figure 3F−H). However, solutions of poly-**3*β***, poly-**1α**, and poly-**1*γ*** did not form a gel even after 1 week (Table S1 in the Supporting Information), suggesting that the chiral solvation through the cooperative interaction of **4** with the linker residues of the CyD-bound poly(phenylacetylene)s as well as a favorable enantioselective inclusion complexation of **4** into the *β*-CyD cavity seem to be essential for the formation of a gel. However, the enantioselectivity of **4** with *β*-CyD derivatives was reported to be poor[12,13] so that the preferred-handed helical array of the *β*-CyD units and the polar amide (poly-**2*β***) or ester (poly-**1*β***) linker residues along the polymer backbones may play a crucial role for the emergence of such an enantioselective gelation. The gels of poly-**1*β*** and poly-**2*β*** prepared in water/DMSO (6:4, v/v) with (*S*)-**4** ([**4**]/[polymer] = 40, [polymer] = 20 mg/mL) exhibited characteristic ICDs, but the ICD intensities decreased with an increase in the temperature and almost completely disappeared after melting at 50 and 60 °C, respectively. These gel−sol transitions accompanied by the ICD changes reversibly took place (Figure 4). These results suggest that a preferred-handed helical conformation of the polymers may be necessary for the gelation.

Poly-**2*β*** did not form a gel in water/DMSO (6/4, v/v) containing (*S*)-**4** (([**4**]/[poly-**2*β***] = 40−1000) when the poly-**2*β*** concentration was 1 mg/mL. Unprecedentedly, we found a small amount of precipitate after the solution had been allowed to stand for 5 days, whereas no precipitation occurred for poly-**2*β*** with (*R*)-**4**. AFM images of poly-**2*β*** cast from a dilute solution of poly-**2*β*** (0.1 mg/mL) in water/DMSO (6:4, v/v) containing (*S*)-**4** ([(*S*)-**4**]/[poly-**2*β***] = 300) on mica after the sample had been allowed to stand for hours revealed individual poly-**2*β*** chains after 2 h, but aggregated large particles were observed after 24 h (Figure S3 in the Supporting Information). These results suggest that poly-**2*β*** gradually aggregates with time in the solvent with (*S*)-**4** and finally forms a fibril-like helical morphology through hierarchical self-assembly. By measuring the AFM images of the individual poly-**2*β*** chains, we estimated the number-average molecular length (L_n) and average height to be 15.7 and 1.8 ± 0.16 nm, respectively, based on an evaluation of ca. 100 molecules. The SEM images of the precipitates after sputter-coating with gold clearly revealed right-handed twisted rod-like ribbon structures (Figure 5A,C) with a diameter of a few micrometers and a length of >100 μm. Quite interestingly, some of them formed double helices, and each strand also appeared to be predominantly right-handed (Figure 5A,B). The expanded SEM image of the open-ended cross section indicates that the helical aggregates may not be tubular in morphology (Figure 5D). As a consequence, the chirality of (*S*)-**4** biased the preference of the helical poly-**2*β*** for the formation of a micrometer-scale, right-handed superstructured helix.

Similar supramolecular aggregates could be obtained when a solution of poly-**2*β*** in water/DMSO mixture (1 mg/mL; 6:4, v/v) was slowly evaporated under reduced pressure on a tilted glass plate (Figure 5E), resulting in fibril-like helical aggregates independent of the presence and absence of (*S*)-**4**, and right-handed twisted aggregates could be partially observed. Other CyD-bound poly(phenylacetylene)s (poly-**1*β***, poly-**3*β***, poly-**1α**, and poly-**1*γ***) also formed fibril-like aggregates (Figure 6), in which only poly-**1*β*** partially formed a twisted aggregate in a hierarchical fashion, although its helical structure and

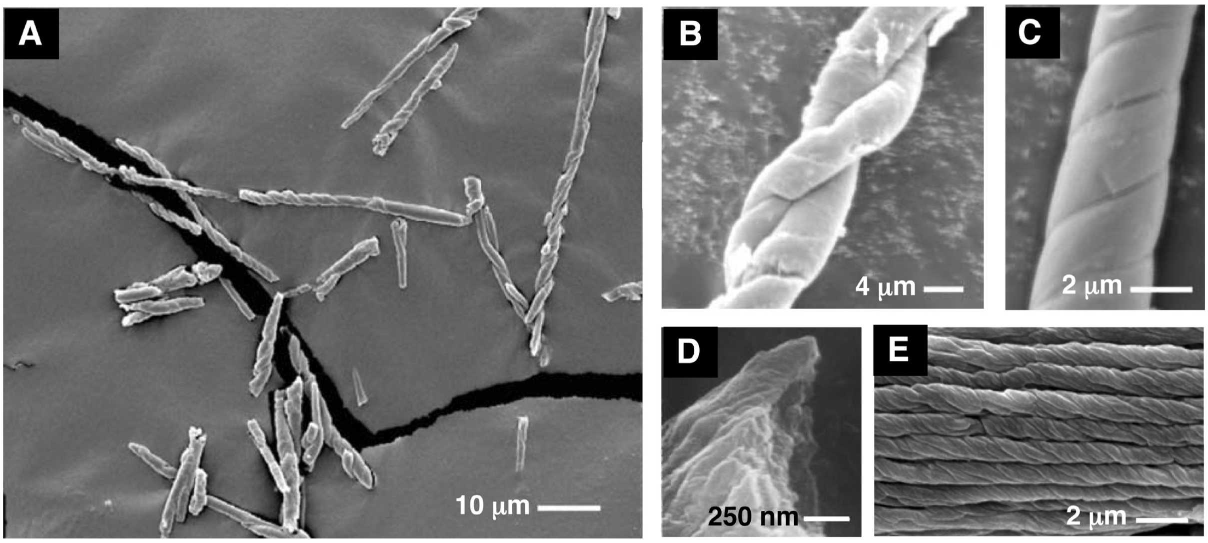

Figure 5. SEM images of self-assembled helical poly-**2*β*** aggregates obtained from slow evaporation of a solution of poly-**2*β*** (1 mg/mL) in water/DMSO (6:4, v/v) in the presence (A–D) and absence (E) of (*S*)-**4** ([(*S*)-**4**]:[poly-**2*β***] 1000:1, mol/mol). The open-ended cross-section of aggregates (D) and side views of an individual helical poly-**2*β*** aggregate (A–C) and multiple fibril-like aggregates (E) are shown.

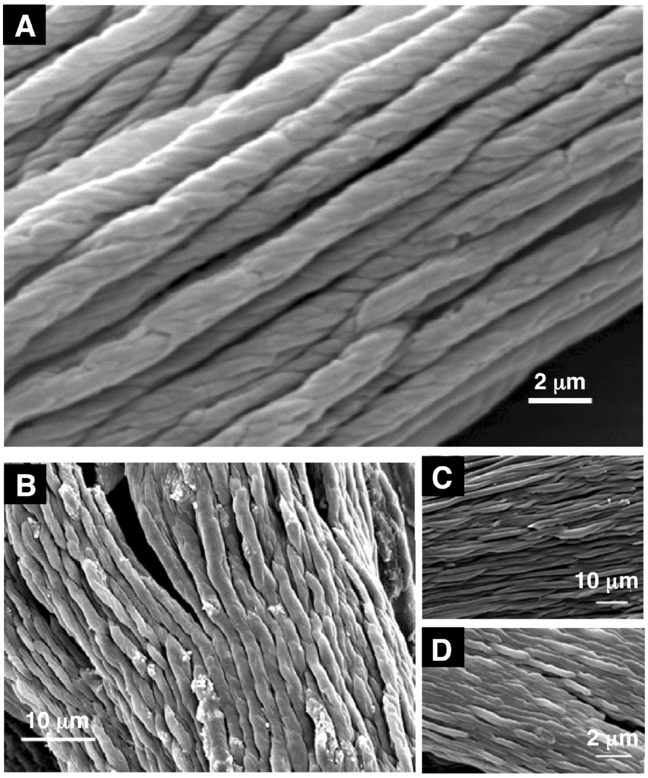

Figure 6. SEM images of self-assembled poly-**1*β*** (A), poly-**3*β*** (B), poly-**1α** (C), and poly-**1*γ*** (D) aggregates prepared from a DMSO/water (4:6, v/v) solution (1 mg/mL) onto a tilted glass plate by slowly evaporating the solvent under reduced pressure.

handedness were not completely uniform and one-handed. These SEM observations suggest that the CyD-bound poly(phenylacetylene)s tend to form unique micrometer-scale fibril-like arrays, and poly-**1*β*** and poly-**2*β*** with a *β*-CyD pendant connected through a polar amide or ester linkage self-aggregate to form twisted ribbon structures biased by the chiral CyD residues. The biased preference for one particular helical sense may possibly be amplified in the presence of (*S*)-**4**.

CONCLUSIONS

In summary, we found that the linkage groups of the *β*-CyD-bound helical poly(phenylacetylene)s play a crucial role in the conformational change induced by external stimuli, such as the temperature, solvent, and chirality. In addition, we demonstrated that poly-**1*β*** and poly-**2*β*** with a *β*-CyD pendant connected through polar amide and ester linkages, respectively, showed a unique enantioselective gelation in response to the chirality of the chiral amine (**4**), and the polymers further formed hierarchical superstructured helical assemblies on a micrometer scale with a controlled helix-sense, as evidenced by the SEM observations. We note that hierarchical superstructured helix formation through self-assemblies of synthetic helical polymers is quite rare,[4] although a large number of helical aggregates with a well-defined structure has been constructed from small molecules based on self-assembly, supramolecular assembly through non-covalent interactions, or both.[1,2] The detailed mechanism for such a specific gelation and micrometer-scale superstructured helix formation observed for the particular CyD-bound poly(phenylacetylene)s is not completely understood at present, but these helical systems will contribute to the design and synthesis of new stimuli-responsive helical polymers with greater sensitivity accompanied by a visible[6] or fluorescence color change[14] and also provide intriguing potentials for applications in future smart chiral materials for chiral recognition[8,15] and enantioselective catalysis.[8,16]

EXPERIMENTAL SECTION

Instruments. NMR spectra were measured on a Varian Mercury-300 spectrometer operating at 300 MHz for ^{1}H with TMS (for $CDCl_3$) or a solvent residual peak (for DMSO-d_6) as the internal standard. IR spectra were recorded using a JASCO Fourier transform IR-620 spectrophotometer (Hachioji, Japan). Optical rotation was measured on a JASCO P-1030 polarimeter in a 5 or 1 cm quartz cell at 25 °C equipped with a temperature controller (EYELA NCB-2100, Tokyo, Japan). Absorption and CD spectra were measured in a 0.1 cm quartz cell unless otherwise noted using a JASCO V-570 spectrophotometer and JASCO J-725 or JASCO J-820 spectropolarimeter, respectively. Temperature was controlled with a JASCO PTC-348WI or PTC-423 L and an ETC-505T apparatus for CD and absorption measurements, respectively. The concentrations of polymers were calculated based on the monomer units and were 1 mg/mL unless otherwise stated. SEC was performed using a JASCO PU-980 liquid chromatograph equipped with a UV−visible detector (254 nm; JASCO UV-970), an RI detector (JASCO RI-930), and a column oven (JASCO CO-965). The molecular weights of polymers were determined at 40 °C using Tosoh TSKgel α-3000 (30 cm) and α-5000 (30 cm) SEC columns connected in series, and DMF containing 10 mM LiCl was used as the eluent at a flow rate of 0.5 mL/min. The molecular weight calibration curve was obtained with poly(ethylene oxide) (PEO) and poly(ethylene glycol) (PEG) standards (Tosoh). Laser Raman spectra were measured on a JASCO RMP-200 spectrophotometer. Matrix-assisted laser desorption/ionization time-of-flight mass (MALDI-TOF MS) spectra were recorded on a Voyager-DE STR (PerSeptive Biosystems) using α-cyano-4-hydroxycinnamic acid or glycerol as the matrix. SEM measurements were performed on a JEOL JMS-5600 or a HITACHI S-5000 SEM with the accelerating voltage of 10 kV and emission current of 10 μA. AFM measurements were performed using a Nanoscope IIIa microscope (Veeco Instruments, Santa Barbara, CA) in air at ambient temperature with standard silicon cantilevers (NCH, Nanoworld, Neuchâtel, Switzerland) in the tapping mode. The AFM images were measured at the resonance frequency of the tips with 125 μm long cantilevers (200−300 Hz) and a spring constant of ~40 N/m. All images were collected with the maximum available number of pixels (512) in each direction. The scanning speed was at a line frequency of 1.0 Hz.

Materials. DMF and DMSO were dried over calcium hydride and distilled under reduced pressure. Triethylamine (Et_3N) was distilled and dried over KOH pellets under nitrogen. [(Norbornadiene)rhodium(I) chloride]$_2$ ([Rh(nbd)Cl]$_2$) was purchased from Aldrich and used as received. β-CyD and *p*-toluenesulfonylchloride were obtained from Kishida (Osaka, Japan). (4-Carboxyphenyl)acetylene (CPA)[17] and 4-[2-(trimethylsilyl)ethynyl]phenol[18] were prepared according to the previously reported methods. (*R*)- and (*S*)-1-Phenylethylamine (**4**) were kindly supplied from Yamakawa Chemical (Tokyo, Japan). Two novel phenylacetylenes, [(6-β-CyD)carboxyphenyl]acetylene (**2*β***) and [(6-β-CyD)oxyphenyl]acetylene (**3*β***), were synthesized according to Scheme 1. CyD-bound poly(phenylacetylene)s (poly-**1*β***−poly-**3*β***, poly-**1α**, and poly-**1*γ***) were synthesized according to the previously reported method,[5,7] and their M_n and M_w/M_n values are summarized in Table 1.

Mono-6-deoxy-6-toluenesulfonyl-*β*-cyclodextrin (*β*-Tos-CyD). This compound was prepared from β-CyD and *p*-toluenesulfonylchloride according to the literature method.[19] The yield was 14.7% based on β-CyD. ^{1}H NMR (300 MHz, DMSO-d_6): δ 2.43 (s, 3H; Ar−CH_3), 3.19−3.78 (m, 42H; CH and CH_2), 4.14−4.58 (m, 6H; OH), 4.72−4.94 (m, 7H; CH), 5.60−5.88 (m, 14H; OH), 7.24 (d, 2H; aromatic), 7.77 (d, 2H; aromatic).

Sodium Salt of CPA (CPA-Na). To a suspension of CPA (2.2 g, 15.1 mmol) in water (275 mL) was added 1.0 N NaOH aqueous solution (13.5 mL, 13.5 mmol), and the mixture was stirred at room temperature overnight. After filtration, the filtrate was lyophilized to give CPA-Na (1.87 g, 11.2 mmol) in 74% yield. This compound was used for the next reaction without further purification.

[(6-*β*-CyD)carboxyphenyl]acetylene (2*β*). To a solution of β-Tos-CyD (10.3 g, 7.97 mmol) in DMSO (150 mL) was added CPA-Na (1.71 g, 10.2 mmol), and the mixture was stirred at 80 °C. After 46 h, the reaction mixture was allowed to cool to room temperature and poured in a large amount of acetone. The resulting precipitate was collected by filtration, washed with water, and dried in vacuo at room temperature overnight to give pure **2*β*** (5.89 g, 4.67 mmol) in 59% yield as a white powder. Mp > 300 °C. $[\alpha]_D^{25}$ +130.9 (*c* 0.5, DMSO). IR (nujol, cm^{-1}): 2106 (C≡C), 1718 (C═O of ester). ^{1}H NMR (300 MHz, DMSO-d_6): δ 3.20−3.90 (m, 36H; CH and CH_2), 4.31−4.95 (m, 12H; OH and ≡CH), 5.37−5.63 (m, 12H; OH), 7.62 (d, *J* = 8.1 Hz, 2H; aromatic), 7.98 (d, *J* = 8.4 Hz, 2H; aromatic). MALDI-TOF MS: m/z = 1263 [**2*β*** + H]$^+$. Anal. calcd (%) for $C_{51}H_{74}O_{36}\cdot 4H_2O$: C, 45.88; H, 6.19. Found: C, 45.84; H, 6.32.

[(6-*β*-CyD)oxyphenyl]acetylene (3*β*). To a solution of β-Tos-CyD (3.38 g, 2.62 mmol) in DMF (70 mL) was added 4-[2-(trimethylsilyl)ethynyl]phenol (0.50 g, 2.62 mmol) and potassium carbonate (0.36 g, 2.60 mmol), and the mixture was stirred at 80 °C. After 14 h, the reaction mixture was allowed to cool to room temperature and then poured in a large amount of acetone. The resulting precipitate was collected by filtration, washed with water, and dried in vacuo at room temperature overnight. The crude **3*β*** was purified by a column chromatography charged with Diaion HP-20 with water/methanol (10:0 to 6:4, v/v) as the eluent to give pure **3*β*** (0.65 g, 0.52 mmol) in 20% yield as a white solid. Mp > 300 °C. $[\alpha]_D^{25}$ +142.2 (*c* 0.5, DMSO). IR (nujol, cm^{-1}): 2101 (C≡C). ^{1}H NMR (300 MHz, DMSO-d_6): δ 3.20 − 3.78 (m, 36H; CH and CH_2), 4.31−4.95 (m, 12H; OH and ≡CH), 5.37−5.63 (m, 12H; OH), 6.94 (d, *J* = 9.3 Hz, 2H; aromatic), 7.37 (d, *J* = 8.7 Hz, 2H; aromatic). MALDI-TOF MS: m/z = 1236 [**3*β*** + H]$^+$. Anal. calcd (%) for $C_{50}H_{74}O_{35}\cdot 3H_2O$: C, 46.58; H, 6.25. Found: C, 46.53; H, 6.31.

Polymerization. Polymerization was carried out in a dry ampule under a dry nitrogen atmosphere using [Rh(nbd)Cl]$_2$ as a catalyst according to Scheme 1. A typical polymerization procedure is described below.

Poly-2*β*. **2*β*** (1.51 g, 1.20 mmol) was placed in a dry ampule, which was then evacuated on a vacuum line and flushed with dry nitrogen, and a three-way stopcock was attached to the ampule. DMF (7.7 mL) was added with a syringe, and **2*β*** was dissolved completely and Et_3N (1.7 mL) was added. To this monomer solution was added a solution of [Rh(nbd)Cl]$_2$ in DMF at 30 °C. The concentrations of the monomer and the rhodium catalyst were 0.1 and 0.001 M, respectively. The color of the mixture changed to reddish brown, and the solution became viscous within 10 min. After 17 h, the resulting polymer was precipitated in a large amount of methanol, collected by centrifugation, and dried in vacuo at 50 °C for 2 h (1.64 g, quantitative). The SEC measurement of the obtained methanol insoluble fraction showed a bimodal SEC trace, suggesting that the poly-**2*β*** consisted of two fractions, a high-molecular-weight polymeric fraction and a low-molecular-weight oligomeric fraction. To remove the low-molecular-weight fraction, we dissolved the methanol insoluble part in DMSO (100 mL) and added methanol (100 mL) as a poor solvent. The resulting yellow precipitate was collected by centrifugation and washed with methanol. This reprecipitation procedure was repeated two times. The fractionated polymer was then dried in vacuo at 50 °C for 2 h to give poly-**2*β*** showing a unimodal SEC trace (0.69 g, 45% yield). Poly-**2*β*** was soluble in DMSO, DMF, and water but insoluble in other common organic solvents, such as toluene, THF, $CHCl_3$, acetonitrile, and acetone. The M_n and M_w/M_n of the poly-**2*β*** were estimated to be 8.1 × 10^4 and 1.2, respectively, as determined by SEC (PEO and PEG standards using DMF containing 10 mM LiCl as the eluent). The elemental analysis of the polymer agreed satisfactorily with the calculated values. The stereoregularity of the poly-**2*β*** was investigated by NMR and Raman spectroscopies. However, we could not estimate the stereoregularity of the poly-**2*β*** by its ^{1}H NMR spectrum because of the broadening of the main chain protons and the overlapping with some CyD protons even at 80 °C. The Raman spectrum of poly-**2*β*** gave useful information and showed intense peaks at 1547, 1335, and 963 cm^{-1}, which can be assigned to the C═C, C−C, and C−H bond vibrations in the *cis*-polyacetylenes,[20] whereas those in the *trans*-polyacetylene were not observed, indicating that the poly-**2*β*** possesses a highly cis−transoidal structure (Figure S1 in the Supporting Information).[21]

*Spectroscopic Data of Poly-**2β**.* $[\alpha]_D^{25}$ +1102 (*c* 0.1, DMSO), +165 (*c* 0.1, water). IR (KBr, cm^{-1}): 1718 cm^{-1} (C═O of ester). Anal. calcd (%) for $(C_{51}H_{74}NO_{36}\cdot 5H_2O)_n$: C, 45.27; H, 6.26. Found: C, 45.18; H, 6.25.

Poly-3*β*. This polymer was prepared according to an analogous method for the synthesis of poly-**2*β***. The obtained methanol-insoluble fraction also consisted of a high-molecular-weight polymer and a low-molecular-weight oligomer. To remove the low-molecular-weight oligomer, we dissolved the methanol-insoluble part in DMSO and added methanol as a poor solvent. The resulting yellow precipitate was collected by centrifugation and washed with methanol. This procedure was repeated twice. The fractionated polymer was dried in vacuo at 50 °C for 2 h to give poly-**3*β*** showing a unimodal SEC trace (0.31 g, 61% yield). Poly-**3*β*** was soluble in DMSO, DMF, and alkaline water (pH >10). The M_n and M_w/M_n of the poly-**3*β*** were estimated to be 9.6×10^4 and 1.2, respectively, as determined by SEC (PEO and PEG standards using DMF containing 10 mM LiCl as the eluent).

*Spectroscopic Data of Poly-**3β**.* $[\alpha]_D^{25}$ −585 (*c* 0.1, DMSO), −25 (*c* 0.1, alkaline water (pH 10.5)). Anal. calcd (%) for $(C_{50}H_{74}O_{35}\cdot 7H_2O)_n$: C, 44.12; H, 6.52. Found: C, 44.27; H, 6.61.

CD Measurements: Effect of H_2O on CD of Poly-2*β* and Poly-3*β*. A typical experimental procedure for poly-**2*β*** is described below. A solution of poly-**2*β*** (2 mg/mL) in DMSO was prepared in six 1 mL flasks equipped with stopcocks. To each flask was added deionized, degassed H_2O (50, 100, 150, 200, and 300 μL) using a Hamilton microsyringe, respectively, and the solutions were diluted with DMSO so as to keep the poly-**2*β*** concentration to be 1.0 mg/mL. Absorption and CD spectra were then taken for each flask at various temperatures controlled with a thermocontroller. In a similar manner, effect of H_2O on CD of poly-**3*β*** was investigated.

Effect of Chiral Amine (4) on CD of Poly-2*β* and Poly-3*β*. A typical experimental procedure for poly-**2*β*** is described below. A stock solution of poly-**2*β*** (2.5 mg/mL) in DMSO was prepared in a 1 mL flask equipped with a stopcock. A 400 μL aliquot of the stock solution of poly-**2*β*** was transferred to two 1 mL flasks equipped with stopcocks, and 600 μL of deionized, degassed water was added to each flask using a Hamilton microsyringe so as to keep the poly-**2*β*** concentration to be 1.0 mg/mL. To each flask was added 30 μL of (*S*)- and (*R*)-**4**, and the absorption and CD spectra were then taken for each flask at 25 °C. The same procedure was performed in the experiments with poly-**3*β*** using (*S*)- and (*R*)-**4**.

Enantioselective Gelation. A typical experimental procedure is described below. Poly-**2*β*** (*ca.* 4.0 mg, 3.2 μmol) was placed in ten vessels and a 20 μL aliquot of DMSO was then added to each vessel. After complete dissolution of the poly-**2*β***, the solutions were diluted with appropriate amounts of DMSO then water so as to keep the water contents (vol %) (0, 10, 20, 30, 40, 50, 60, 70, 80, and 90) and the poly-**2*β*** concentration at 20 mg/mL. To each vessel was added 16 μL of (*S*)- or (*R*)-**4** (128 μmol) with a Hamilton microsyringe, and the solutions were immediately mixed with a vibrator. The same procedures were performed in the experiments with poly-**1*β***, poly-**3*β***, poly-**1α**, and poly-**1*γ*** (Table S1 in the Supporting Information).

AFM Measurements of Gel. An organogel of poly-**2*β*** was prepared in the same way as that described above in water/DMSO (6:4 v/v) in the presence of (*S*)-**4** ([poly-**2*β***] = 20 mg/mL, [(*S*)-**4**]/[poly-**2*β***] = 40). A freshly cleaved HOPG was placed on the gel; then, surface layers were transferred by peeling off the HOPG substrate.[11] After the sample was dried under vacuum for 2 h, the AFM measurement was performed in air at ambient temperature in the tapping mode (Figure 3E).

AFM Measurements of Poly-2*β* Prepared in Solution with (*S*)-4. A stock solution of poly-**2*β*** (0.1 mg/mL) in water/DMSO (6/4, v/v) containing (*S*)-**4** ([(*S*)-**4**]/[poly-**2*β***] = 300) was prepared. After the sample had been allowed to stand for 2 and 24 h, a 10 μL aliquot of the stock solution was dropped on a freshly cleaved mica, the solution was simultaneously blown off with a stream of nitrogen, then the mica substrate was dried in vacuo overnight to measure the AFM images in the tapping mode (Figure S3 in the Supporting Information).

SEM Observations of Helically Assembled Poly-2*β* Prepared in Solution with (*S*)-4. A stock solution of poly-**2*β*** (1 mg/mL) in water/DMSO (6:4 v/v) containing an excess amount of (*S*)-**4** ([(*S*)-**4**]/[poly-**2*β***] = 1000) was prepared in a vessel with a screw cap. After the solution had been allowed to stand at room temperature (ca. 20−25 °C) for 2 days, the solvent was slowly removed by evaporation under reduced pressure in a desiccator. The residual solid was scratched out with a spatula and mounted on copper stubs with a double-sided conductive carbon tape. The sample was then sputter-coated with gold under an electric current of 20 mA at 8 Pa for 20 s before SEM measurements.

SEM Observations of Self-Assembled CyD-bound Poly(phenylacetylene)s Prepared in Solutions without (*S*)-4. A typical procedure is described below. A solution of poly-**2*β*** (0.1 mg/mL) in water/DMSO (6:4, v/v) was prepared in a vessel with a screw cap. A glass plate was vertically placed in the vessel. and the solvent was slowly removed by evaporation under reduced pressure in a desiccator. The film formed on the glass surface after removal of the solvent was peeled off using a razor and mounted on copper stubs with a double-sided conductive carbon tape. The sample was then sputter-coated with gold under an electric current of 20 mA at 8 Pa for 20 s before SEM measurements. The same procedures were performed in the experiments with poly-**1*β***, poly-**3*β***, poly-**1α**, and poly-**1*γ***.

■ ASSOCIATED CONTENT

Ⓢ Supporting Information. Raman spectra of poly-**2*β*** and poly-**3*β***, CD and UV/vis spectral changes of poly-**1*β*** with visible color changes induced by external stimuli, solvent effects on gelation of CyD-bound poly(phenylacetylene)s, and AFM images of poly-**2*β*** with (*S*)-**4** deposited on mica. This material is available free of charge via the Internet at http://pubs.acs.org.

■ AUTHOR INFORMATION

Corresponding Author

*E-mail: yashima@apchem.nagoya-u.ac.jp.

Present Addresses

[†]Graduate School of Natural Science and Technology, Kanazawa University, Kakuma-machi, Kanazawa 920-1192, Japan.

■ ACKNOWLEDGMENT

This work was partially supported by Grant-in-Aid for Scientific Research (S) from the Japan Society for the Promotion of Science (JSPS).

■ REFERENCES

(1) For recent reviews of supramolecular helical assemblies based on small molecules, see: (a) Rowan, A. E.; Nolte, R. J. M. *Angew. Chem., Int. Ed.* **1998**, *37*, 63–68. (b) Lee, M.; Cho, B.-K.; Zin, W.-C. *Chem. Rev.* **2001**, *101*, 3869–3892. (c) Brunsveld, L.; Folmer, B. J. B.; Meijer, E. W.; Sijbesma, R. P. *Chem. Rev.* **2001**, *101*, 4071–4097. (d) van Bommel, K. J. C.; Friggeri, A.; Shinkai, S. *Angew. Chem., Int. Ed.* **2003**, *42*, 980–999. (e) Elemans, J. A. A. W.; Rowan, A. E.; Nolte, R. J. M. *J. Mater. Chem.* **2003**, *13*, 2661–2670. (f) Shimizu, T.; Masuda, M.; Minamikawa, H. *Chem. Rev.* **2005**, *105*, 1401–1444. (g) Keizer, H. M.; Sijbesma, R. P.

Chem. Soc. Rev. **2005**, *34*, 226–234. (h) You, C.-C.; Dobrawa, R.; Saha-Möller, C. R.; Würthner, F. *Top. Curr. Chem.* **2005**, *258*, 39–82. (i) Ajayaghosh, A.; George, S. J.; Schenning, A. P. H. J. *Top. Curr. Chem.* **2005**, *258*, 83–118. (j) Maeda, K.; Yashima, E. *Top. Curr. Chem.* **2006**, *265*, 47–88. (k) Palmans, A. R. A.; Meijer, E. W. *Angew. Chem., Int. Ed.* **2007**, *46*, 8948–8968. (l) Pijper, D.; Feringa, B. L. *Soft Matter* **2008**, *4*, 1349–1372. (m) Kim, H.-J.; Lim, Y.-B.; Lee, M. *J. Polym. Sci., Part A: Polym. Chem.* **2008**, *46*, 1925–1935. (n) Rosen, B. M.; Wilson, C. J.; Wilson, D. A.; Peterca, M.; Imam, M. R.; Percec, V. *Chem. Rev.* **2009**, *109*, 6275–6540.

(2) For selective references of supramolecular helical assemblies based on small molecules, see: (a) Gulik-Krzywicki, T.; Fouquey, C.; Lehn, J.-M. *Proc. Natl. Acad. Sci., U.S.A.* **1993**, *90*, 163–167. (b) Fenniri, H.; Mathivanan, P.; Vidale, K. L.; Sherman, D. M.; Hallenga, K.; Wood, K. V.; Stowell, J. G. *J. Am. Chem. Soc.* **2001**, *123*, 3854–3855. (c) George, S. J.; Ajayaghosh, A.; Jonkheijm, P; Schenning, A. P. H. J.; Meijer, E. W. *Angew. Chem., Int. Ed.* **2004**, *43*, 3422–3425. (d) Percec, V.; Dulcey, A. E.; Balagurusamy, V. S. K.; Miura, Y.; Smidrkal, J.; Peterca, M.; Nummelin, S.; Edlund, U.; Hudson, S. D.; Heiney, P. A.; Duan, H.; Maganov, S. N.; Vinogradov, S. A. *Nature* **2004**, *430*, 764–768. (e) Jin, W.; Fukushima, T.; Niki, M.; Kosaka, A.; Ishii, N.; Aida, T. *Proc. Natl. Acad. Sci., U.S.A.* **2005**, *102*, 10801–10806. (f) Messmore, B. W.; Sukerkar, P. A.; Stupp, S. I. *J. Am. Chem. Soc.* **2005**, *127*, 7992–7993. (g) Bae, J.; Choi, J.-H.; Yoo, Y.-S.; Oh, N.-K.; Kim, B.-S.; Lee, M. *J. Am. Chem. Soc.* **2005**, *127*, 9668–9669. (h) Brizard, A.; Aimé, C.; Labrot, T.; Huc, I.; Berthier, D.; Artzner, F.; Desbat, B.; Oda, R. *J. Am. Chem. Soc.* **2007**, *129*, 3754–3762. (i) Jin, W.; Yamamoto, Y.; Fukushima, T.; Ishii, N.; Kim, J.; Kato, K.; Takata, M.; Aida, T. *J. Am. Chem. Soc.* **2008**, *130*, 9434–9440. (j) Smulders, M. M. J.; Filot, I. A. W.; Leenders, J. M. A.; van der Schoot, P.; Palmans, A. R. A.; Schenning, A. P. H. J.; Meijer, E. W. *J. Am. Chem. Soc.* **2010**, *132*, 611–619. (k) Murnen, H. K.; Rosales, A. M.; Jaworski, J. N.; Segalman, R. A.; Zuckermann, R. N. *J. Am. Chem. Soc.* **2010**, *132*, 16112–16119.

(3) For recent examples, see: (a) Ionescu-Zanetti, C.; Khurana, R.; Gillespie, J. R.; Petrick, J. S.; Trabachino, L. C.; Minert, L. J.; Carter, S. A.; Fink, A. L. *Proc. Natl. Acad. Sci., U.S.A.* **1999**, *96*, 13175–13179. (b) Jiménez, J. L.; Nettleton, E. J.; Bouchard, M.; Robinson, C. V.; Dobson, C. M.; Saibil, H. R. *Proc. Natl. Acad. Sci., U.S. A.* **2002**, *99*, 9196–9201. (c) Rubin, N.; Perugia, E.; Goldschmidt, M.; Fridkin, M.; Addadi, L. *J. Am. Chem. Soc.* **2008**, *130*, 4602–4603.

(4) For leading references of supramolecular helical assemblies based on synthetic polymers, see: (a) Cornelissen, J.; Fischer, M.; Sommerdijk, N.; Nolte, R. J. M. *Science* **1998**, *280*, 1427–1430. (b) Li, C. Y.; Cheng, S. Z. D.; Weng, X.; Ge, J. J.; Bai, F.; Zhang, J. Z.; Calhoun, B. H.; Harris, F. W.; Chien, L.-C.; Lotz, B. *J. Am. Chem. Soc.* **2001**, *123*, 2462–2463. (c) Ho, R.-M.; Chiang, Y.-W.; Tsai, C.-C.; Lin, C.-C.; Ko, B.-T.; Huang, B.-H. *J. Am. Chem. Soc.* **2004**, *126*, 2704–2705. (d) Schlaad, H.; Krasia, T.; Antonietti, M. *J. Am. Chem. Soc.* **2004**, *126*, 11307–11310. (e) Koga, T.; Matsuoka, M.; Higashi, N. *J. Am. Chem. Soc.* **2005**, *127*, 17596–17597.

(5) Yashima, E.; Maeda, K.; Sato, O. *J. Am. Chem. Soc.* **2001**, *123*, 8159–8160.

(6) For reviews, see: (a) Okada, S.; Peng, S.; Spevak, W.; Charych, D. *Acc. Chem. Res.* **1998**, *31*, 229–239. (b) Englebienne, P. *J. Mater. Chem.* **1999**, *9*, 1043–1054. (c) McQuade, D. T.; Pullen, A. E.; Swager, T. M. *Chem. Rev.* **2000**, *100*, 2537–2574. (d) Jelinek, R.; Kolusheva, S. *Biotechnol. Adv.* **2001**, *19*, 109–118. (e) Leclerc, M.; Ho, H.-A. *Synlett* **2004**, 380–387. (f) Zheng, J.; Swager, T. M. *Adv. Polym. Sci.* **2005**, *177*, 151–179. (g) Hoeben, F. J. M.; Jonkheijm, P.; Meijer, E. W.; Schenning, A. P. H. J. *Chem. Rev.* **2005**, *105*, 1491–1546.

(7) Maeda, K.; Mochizuki, H.; Watanabe, M.; Yashima, E. *J. Am. Chem. Soc.* **2006**, *128*, 7639–7650.

(8) For leading references of synthetic helical polymers including helix inversion, see: (a) Cheon, K. S.; Selinger, J. V.; Green, M. M. *Angew. Chem., Int. Ed.* **2000**, *39*, 1482–1485. (b) Fujiki, M. *Macromol. Rapid Commun.* **2001**, *22*, 539–563. (c) Nakano, T.; Okamoto, Y. *Chem. Rev.* **2001**, *101*, 4013–4038. (d) Cornelissen, J. J. L. M.; Rowan, A. E.; Nolte, R. J. M.; Sommerdijk, N. A. J. M. *Chem. Rev.* **2001**, *101*, 4039–4070. (e) Nomura, R.; Nakako, H.; Masuda, T. *J. Mol. Catal. A: Chem.* **2002**, *190*, 197–205. (f) Nomura, R.; Tabei, J.; Masuda, T. *Macromolecules* **2002**, *35*, 2955–2961. (g) Lam, J. W. Y.; Tang, B. Z. *Acc. Chem. Res.* **2005**, *38*, 745–754. (h) Sinkeldam, R. W.; van Houtem, M. H. C. J.; Pieterse, K.; Vekemans, J. A. J. M.; Meijer, E. W. *Chem.—Eur. J.* **2006**, *12*, 6129–6137. (i) Pijper, D.; Feringa, B. L. *Angew. Chem., Int. Ed.* **2007**, *46*, 3693–3696. (j) Yashima, E.; Maeda, K. *Macromolecules* **2008**, *41*, 3–12. (k) Yashima, E.; Maeda, K.; Furusho, Y. *Acc. Chem. Res.* **2008**, *41*, 1166–1180. (l) Rudick, J. G.; Percec, V. *Acc. Chem. Res.* **2008**, *41*, 1641–1652. (m) Liu, J.; Lam, J. W. Y.; Tang, B. Z. *Chem. Rev.* **2009**, *109*, 5799–5867. (n) Yashima, E.; Maeda, K.; Iida, H.; Furusho, Y.; Nagai, K. *Chem. Rev.* **2009**, *109*, 6102–6211. (o) Fujiki, M. *Chem. Rec.* **2009**, *9*, 271–298. (p) Yashima, E. *Polym. J.* **2010**, *42*, 3–16. (q) Schwartz, E.; Koepf, M.; Kitto, H. J.; Nolte, R. J. M.; Rowan, A. E. *Polym. Chem.* **2011**, *2*, 33–47.

(9) For leading references of colorimetric chiral recognition, see: (a) Nishi, T.; Ikeda, A.; Matsuda, T.; Shinkai, S. *J. Chem. Soc., Chem. Commun.* **1991**, 339–341. (b) Yamamoto, K.; Isoue, K.; Sakata, Y.; Kaneda, T. *J. Chem. Soc., Chem. Commun.* **1992**, 791–793. (c) Kubo, Y.; Maeda, S.; Tokita, S.; Kubo, M. *Nature* **1996**, *382*, 522–524. (d) Hirose, K.; Ogasahara, K.; Nishioka, K.; Tobe, Y.; Naemura, K. *J. Chem. Soc., Perkin Trans. 2* **2000**, 1984–1993. (e) Korbel, G. A.; Lalic, G.; Shair, M. D. *J. Am. Chem. Soc.* **2001**, *123*, 361–362. (f) van Delden, R. A.; Feringa, B. L. *Angew. Chem., Int. Ed.* **2001**, *40*, 3198–3200. (g) Tsubaki, K.; Nuruzzaman, M.; Kusumoto, T.; Hayashi, N.; Bin-Gui, W.; Fuji, K. *Org. Lett.* **2001**, *3*, 4071–4073. (h) Huang, J.; Egan, V. M.; Guo, H.; Yoon, J.-Y.; Briseno, A. L.; Rauda, I. E.; Garrell, R. L.; Knobler, C. M.; Zhou, F.; Kaner, R. B. *Adv. Mater.* **2003**, *15*, 1158–1161. (i) Manesiotis, P.; Hall, A. J.; Emgenbroich, M.; Quaglia, M.; Lorenzi, E. D.; Sellergren, B. *Chem. Commun.* **2004**, 2278–2279. (j) Eelkema, R.; van Delden, R. A.; Feringa, B. L. *Angew. Chem., Int. Ed.* **2004**, *43*, 5013–5016. (k) Zhu, L.; Zhong, Z.; Anslyn, E. V. *J. Am. Chem. Soc.* **2005**, *127*, 4260–4269. (l) Eelkema, R.; Feringa, B. L. *Chem. Asian J.* **2006**, *1*, 367–369. For colorimetric molecular recognition based on helical polymers, see refs 5 and 7 and(m) Otsuka, I.; Hongo, T.; Nakade, H.; Narumi, A.; Sakai, R.; Satoh, T.; Kaga, H.; Kakuchi, T. *Macromolecules* **2007**, *40*, 8930–8937. (n) Kakuchi, R.; Kodama, T.; Shimada, R.; Tago, Y.; Sakai, R.; Satoh, T.; Kakuchi, T. *Macromolecules* **2009**, *42*, 3892–3897.

(10) For enantiomer-selective gelation or sol—gel and gel—sol transitions of supramolecular hydrogels or organogels, see: (a) Zhang, Y.; Gu, H.; Yang, Z.; Xu, B. *J. Am. Chem. Soc.* **2003**, *125*, 13680–13681. (b) Makarevc, J.; Joki, M.; Raza, Z.; Stefanic, Z.; Koji-Prodi, B.; Zinic, M. *Chem.—Eur. J.* **2003**, *9*, 5567–5580. (c) Hirst, A. R.; Smith, D. K.; Feiters, M. C.; Geurts, H. P. M. *Chem.—Eur. J.* **2004**, *10*, 5901–5910. (d) Morino, K.; Oobo, M.; Yashima, E. *Macromolecules* **2005**, *38*, 3461–3468. (e) Zheng, Y.-S.; Ji, A.; Chen, X.-J.; Zhou, J.-L. *Chem. Commun.* **2007**, 3398–3400. (f) Zhou, J.-L.; Chen, X.-J.; Zheng, Y.-S. *Chem. Commun.* **2007**, 5200–5202. (g) Chen, X.; Huang, Z.; Chen, S.-Y.; Li, K.; Yu, X.-Q.; Pu, L. *J. Am. Chem. Soc.* **2010**, *132*, 7297–7299. For chiral stimuli-responsive gels, see:(h) Goto, H.; Zhang, H. Q.; Yashima, E. *J. Am. Chem. Soc.* **2003**, *125*, 2516–2523.

(11) Kimizuka, N.; Shimizu, M.; Fujikawa, S.; Fujimura, K.; Sano, M.; Kunitake, T. *Chem. Lett.* **1998**, 967–968.

(12) (a) Keim, W.; Köhnes, A.; Meltzow, W.; Römer, H. *J. High Resolut. Chromatogr.* **1991**, *14*, 507–527. (b) Nie, M. Y.; Zhou, L. M.; Wang, Q. H.; Zhu, D. Q. *Chromatographia* **2000**, *51*, 736–740. (c) Rekharsky, M.; Inoue, Y. *J. Am. Chem. Soc.* **2000**, *122*, 4418–4435.

(13) The enantiomer-selective adsorption experiments were then carried out to estimate the enantiomeric excess (ee) of **4** adsorbed on poly-**2*β*** along the gelation in the presence of racemic **4**. The amine **4** adsorbed on the poly-**2*β*** was recovered by precipitation in the poor solvent, acetone, followed by desorption of the bound **4** with 1 N HCl aq. The ee value of the adsorbed **4** estimated by chiral HPLC analysis using a chiral column (CROWNPAK CR(+), Daicel) with aqueous $HClO_4$ at pH 1.5 as an eluent was low, 6.5% ((*S*)-rich). This low enantioselectivity of **4** with poly-**2*β*** appears to be in agreement with the reported poor enantioselectivity of **4** with β-CyD derivatives.[12]

(14) Thomas, S. W., III; Joly, G. D.; Swager, T. M. *Chem. Rev.* **2007**, *107*, 1339–1386.

(15) (a) Okamoto, Y.; Yashima, E. *Angew. Chem., Int. Ed.* **1998**, *37*, 1020–1043. (b) Nakano, T. *J. Chromatogr., A* **2001**, *906*, 205–225. (c) Aoki, T.; Kaneko, T. *Polym. J.* **2005**, *37*, 717–735.

(16) (a) Reggelin, M.; Doerr, S.; Klussmann, M.; Schultz, M.; Holbach, M. *Proc. Natl. Acad. Sci., U.S.A.* **2004**, *101*, 5461–5466. (b) Roelfes, G.; Feringa, B. L. *Angew. Chem., Int. Ed.* **2005**, *44*, 3230–3232. (c) Maeda, K.; Tanaka, K.; Morino, K.; Yashima, E. *Macromolecules* **2007**, *40*, 6783–6785. (d) Miyabe, T.; Hase, Y.; Iida, H.; Maeda, K.; Yashima, E. *Chirality* **2009**, *21*, 44–50. (e) Yamamoto, T.; Suginome, M. *Angew. Chem., Int. Ed.* **2009**, *48*, 539–542.

(17) Yashima, E.; Matsushima, T.; Okamoto, Y. *J. Am. Chem. Soc.* **1997**, *119*, 6345–6359.

(18) Yashima, E.; Huang, S. L.; Matsushima, T.; Okamoto, Y. *Macromolecules* **1995**, *28*, 4184–4193.

(19) Hamasaki, K.; Ikeda, H.; Nakamura, A.; Ueno, A.; Toda, F.; Suzuki, I.; Osa, T. *J. Am. Chem. Soc.* **1993**, *115*, 5035–5040.

(20) (a) Shirakawa, H.; Ito, T.; Ikeda, S. *Polym. J.* **1973**, *4*, 460–462. (b) Tabata, M.; Tanaka, Y.; Sadahiro, Y.; Sone, T.; Yokota, K.; Miura, I. *Macromolecules* **1997**, *30*, 5200–5204.

(21) Maeda, K.; Goto, H.; Yashima, E. *Macromolecules* **2001**, *34*, 1160–1164.